Effects of the normalization of projection densities on single particles three-dimensional reconstructions

Luis Gerardo de la Fraga

Sección de Computación

CINVESTAV-IPN. Departamento de Ingeniería Eléctrica

Av. Instituto Politécnico Nacional 2508. 07300 México, D.F.
E-mail: fraga@cs.cinvestav.mx

Abstract

In the process of three-dimensional reconstruction of biological macromolecules, several hundreds, or thousands, of projections are taken from different digitized micrographs (photographs from Electron Microscope). Prior to the reconstruction itself, these projections need to be normalized, by scaling their pixel values properly. Subsequent steps of the process involve classification, location of the projections according to the same reference coordinate system and, finally, the three-dimensional reconstruction of the specimen under study. In this work a new normalization procedure is described. Simulation results of the distorsions produced in the final 3D object by using this different normalization procedure are presented, analyzed and compared to current normalization approaches.

Keywords: density scaling, single particles, three-dimensional reconstruction, visualization, image processing.

1 Introduction

In order to carry out a three-dimensional reconstruction of an object from its two-dimensional projections, the following steps must be solved: (1) the projections must be localized in the same reference coordinate system, or in other words, the Euler angles (θ, φ, ψ) values that describe their orientation must be known. (2) The values of the two coordinates (dx, dy) that describe the location in the projection relative to the origin of the volume coordinate system must also be known. (3) All projections have to be correctly weighted, that is, all they have to belong to the same 3D object. If any of these three

points is not fulfilled, a distorted representation of the 3D object [1, p. 214] would be led.

The starting data for a three-dimensional reconstruction are electron microscopy photographs (so named "micrographs") of a macromolecule preparation whose structure we want to know. On the micrographs we observe many (dozens) of images that we assume, in principle, to be projections of a same structure. To obtain a reconstruction at high resolution levels (< 10 Å) we need thousands of such images. Recently, the 50S ribosome of *E. coli* was resolved at 7.5 Å[2] using 16,000 projections.

In this work we are assuming that points (1), the orientation, and (2), the coordinate system origin, are correct for all projections, and we shall focus on the point (3) about the weighting, or normalization, of all pixels values for each projection.

Van Heel *et. al.* [3] presents an excellent review of all steps involved in single particles 3D reconstruction. General considerations of cryo-electron microscopy in single particles can be seen in [4, 5, 6].

2 Normalization procedures

The general procedure to scale pixels values is to normalize them at a same mean, $\bar{x}$ and standard deviation, σ, using the equation:

$$D_i' = (D_i - \bar{x})/\sigma \tag{1}$$

where D_i' corresponds to the normalized pixel values and D_i are the pixels values of the original image.

Here we going to compare three principal procedures used in the field to normalize:

 1. Carazo *et al* [7] normalize all the projections at a same zero mean

and standard deviation of 1.

2. Radermacher [8] normalizes the projections changing the σ value in Eq. (1) to the mean value of the background of the projection. This background value is calculated over the image border, in a zone free of specimen components.

3. A new procedure in which the values of $\bar{x}$ and σ in Eq. (1) is calculated over the border zone like in the point (2).

The normalization procedure used by Boisset *et al* [9] is reduced to the procedure (3) if we suppose that background (the noise) has a Gaussian distribution [10].

Schatz *et al* [11] normalize all projections as point (1), using a zero mean and an arbitrary variance value of 100. Roseman *et al* [12] simply mention that all projections are normalized at a same mean and standard deviation.

3 Experiment

To study the effects produced by the three different normalization procedures presented in sec. 2 on the final 3D reconstructions, the following experiment was performed:

1. A realistic specimen was constructed: With the atomic model of the bacteriorhodopsin [13] a new lower resolution model was created, at 6 Å, using the program Situs [14] (http://situs.scripps.edu). The resulting volume had a size of 60×57 voxels, with side size of 1.2 Å and was padded with zeros to obtain a cube volume of size 60 voxels by side.

2. A set of $10,361$ projections were created from the specimen. This number of projections correspond to take equispaced samples on the full 3D orientation space at a tilt (the second Euler

angle, φ) of 2° [15], at ranges $0° \leq \theta < 360°$ and $0° \leq \varphi < 180°$. Let this set of projections be named by $P\{\}$. Each projection had a size of 60×60 pixels.

3. A new set of noisy projections, $P_n\{\}$, was created adding Gaussian noise to each projection at a fractional noise level (fnl) [16] of 0.40. The level of noise added to each projection is expressed as the ratio between the standard deviation of the added noise and the average intensity range for all images.

4. Three new sets of projections were created:

   (a) Let $A\{P_n\{\}\}$ the set of projections created from the set of noisy projections and normalized with Carazo *et. al* procedure.

   (b) Let $B\{P_n\{\}\}$ the set created using Radermacher's normalization procedure.

   (c) Let $C\{P_n\{\}\}$ the third set of projections created with the new proposed normalization procedure.

5. Four 3D reconstructions were created using the Algebraic Reconstruction Technique (ART):

   - V_{P_n}, the volume reconstructed from $P_n\{\}$
   - V_A, the second reconstruction obtained from $A\{\}$.
   - V_B, the third volume obtained from $B\{\}$.
   - V_C, the fourth volume obtained from $C\{\}$.

   The projections, 3D reconstructions, and others operations, were carry out with the Xmipp package [17]

4 Results

(a) "Frontal" view

(b) "Lateral" view
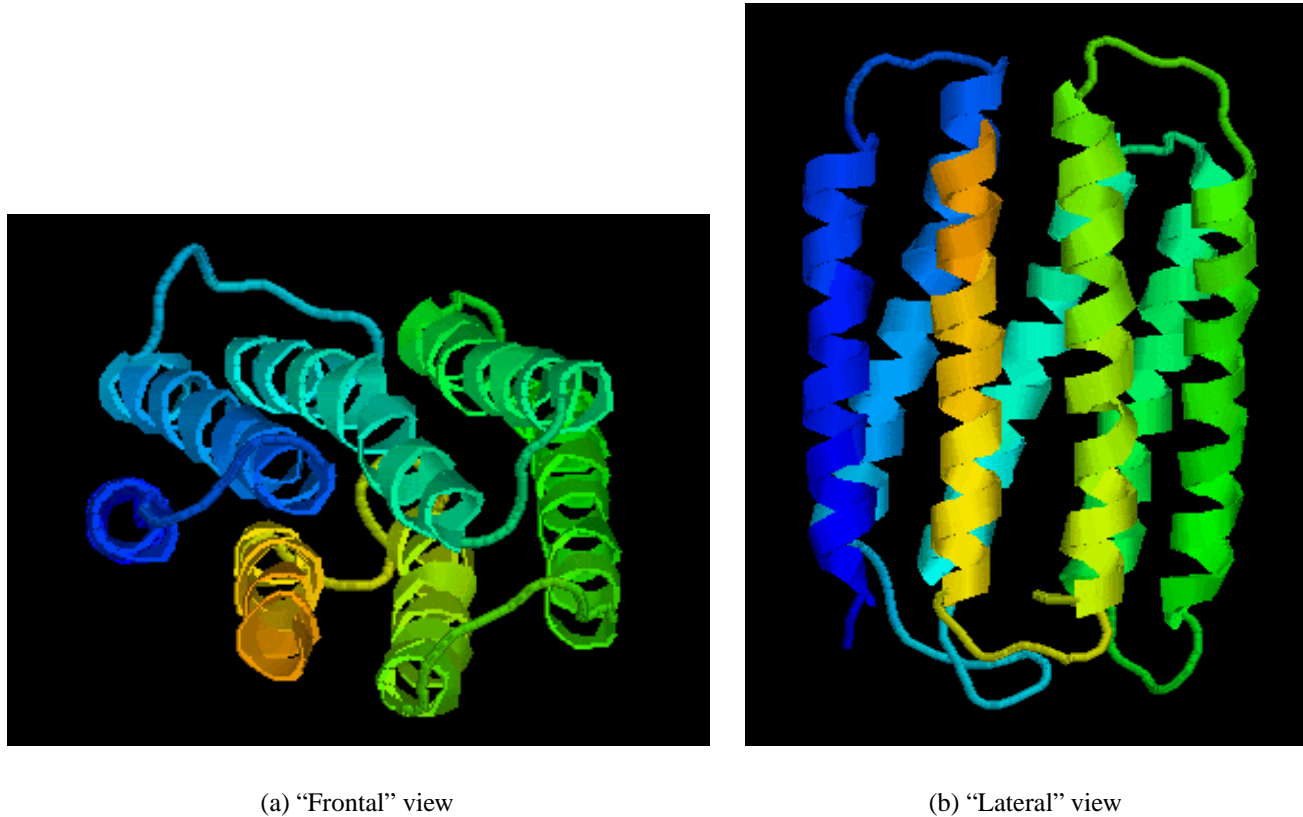
Figure 1: Two images taken from PBD atomic coordinates of the bacteriorhodopsin with *rasmol* program (see http://www.inpharmatica.co.uk/rasmol/).

Acknowledgments

References

[1] J. Frank. *Three-Dimensional Electron Microscopy of Macromolecular Assemblies*. Academic Press, 1996. San Diego, CA.

[2] R. Matadeen, A. Patwardhan abd B. Gowen, E. Orlova, T. Pape, M. Cuff, F. Mueller, R. Brimacombe, and M. van Heel. The *escherichia coli* large ribosomal subunit at 7.5Å resolution. *Structure*, 7:1575–1583, 1999.

[3] M. van Heel, B. Growen, R. Matadeen, E.V. Orlova, R. Finn, T. Pape, D. Cohen, H. Stark, R. Schmidt, M. Schatz, and A. Patwardhan. Single–particle electron cryo–microscopy: towards atomic resolution. *Quartely Reviews of Biophysics*, 33(4):307–369, 2000.

[4] Y. Tao and W. Zhang. Recent developments in cryo-electrom microscopy reconstruction of single particles. *Cur. Op. in Struct. Bio.*, 10:616–622, 2000.

[5] W. Uühlbrandt and K.A. Williams. Analysis of macromolecular structure and dynamics by electron cryo-microscopy. *Cur. Op. in Struct. Bio.*, 3:537–543, 1999.

[6] W. Baumeister and A.C. Steven. Macromolecular electron microscopy in the era of structural genomics. *TIBS*, 25:624–631, 2000.

[7] J.M. Carazo, S. Marco, G. Abella, J.L Carrascosa, J.P. Secilla, and M. Muyal. *J. Struct. Biol*, 106:211–215, 1991.

[8] M. Radermacher. Personal comunication, 2000.

[9] N. Boisset, P. Penczeck, P. François, J. Frank, and J.N. Lamy. Three-dimensional architecture of human α2–macroglobulina transformed with methylamine. *J. Mol. Biol.*, 232:522–529, 1993.

[10] L.G. de la Fraga. Escalamiento en la densidad de imágenes para una reconstrucción tridimensional. In *II Simposium Internacional en Tecnologías Inteligentes, México*, pages 102–108, Oct 2000.

[11] M. Schatz, E.V. Orlova, P. Dube, K. Braig, and M. van Heel. Structure of *lumbricus terrestris* hemoglobin at 30 Å resolution determined using angular reconstitution. *J. Struct. Biol.*, 114:28–40, 1995.

[12] A.M. Roseman, S. Chen, H. Write, K. Braig, and H.R. Saibil. The chaperonin ATPase cycle: mechanism of allosteric switching and movements of substrate-binding domains in GroEL. *Cell*, 87:241–251, 1996.

[13] R. Henderson, J.M. Baldwin, T.A. Ceska, F. Zelmin, E. Beckmann, and K.H. Downing. Model for the structure od bacteriorhodopsin based on high resolution electron cryo-microcope. *J. Mol. Biol.*, 213:899–929, 1990.

[14] W. Wriggers, R.A. Milligan, and J.A. McCammon. Situs; a package for docking crystal structures into low-resolution maps from electrom microscopy. *J. Struct. Biol.*, 125:185–195, 1999.

[15] P. A. Penczek, R. A. Grassuni, and J. Frank. The ribosome at improved resolution: new techniques for for merging and orientation refinement in 3D cryo-electron microscopy of biological particles. *Ultramicroscopy*, 53:251–270, 1994.

[16] N. A. Farrow and F. P. Ottensmeyer. A posteriori determination of relative projection directions of arbitrarily oriented macromolecules. *J. Opt. Soc. Am. A*, 9(10):1749–1760, 1992.

[17] R Marabini, I. M. Masegosa, M. C. San Martin, J.J. Fernández, S. Marco, L. G. de la Fraga, C. Vaquerizo, and J. M. Carazo. Xmipp: An image processing package for electron microscopy. *J. Struct. Biol.*, 116:237–240, 1996.

[18] L.G. de la Fraga and F. Sagols. Scubes: A programa to visualize vox-solids. In *Procedings of Conferencia de Ingeniería Eléctrica 2001, CINVESTAV, México*, 2001. http://www.cs.cinvestav.mx/Scubes.
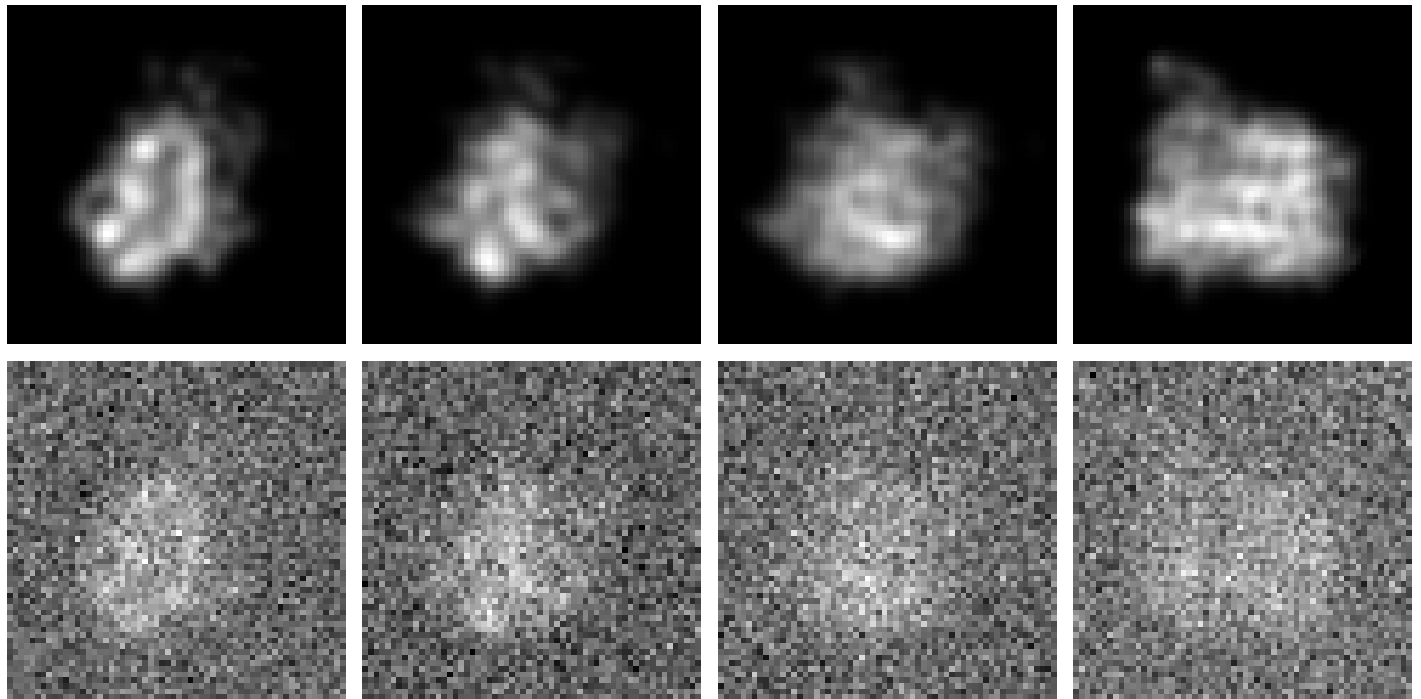
Figure 2: Examples of projections without (top row) and with noise (bottom row)
.
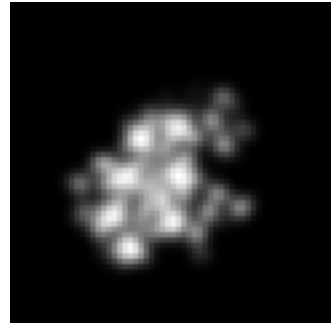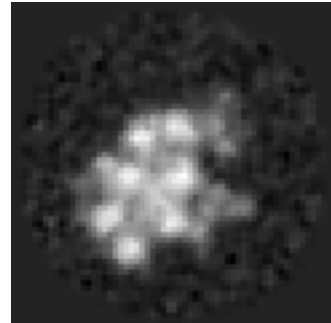
(a) Original   (b) V_{P_n}
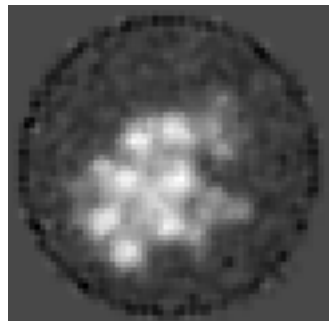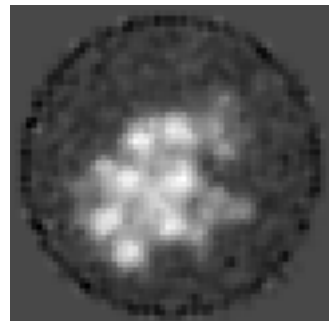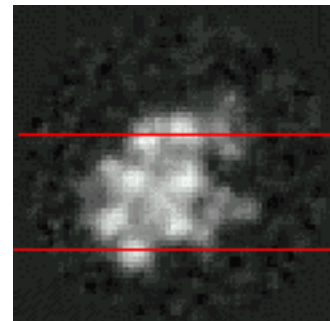
(c) V_A (d) V_B (e) V_C

Figure 3: Images of the slice number 29 (a) of the original specimen, bacteriorhodopsin at a resolution of 6 Å and (b)-(e) of the reconstructed volumes. Image (e) shows two red lines which values are presented in next figures.
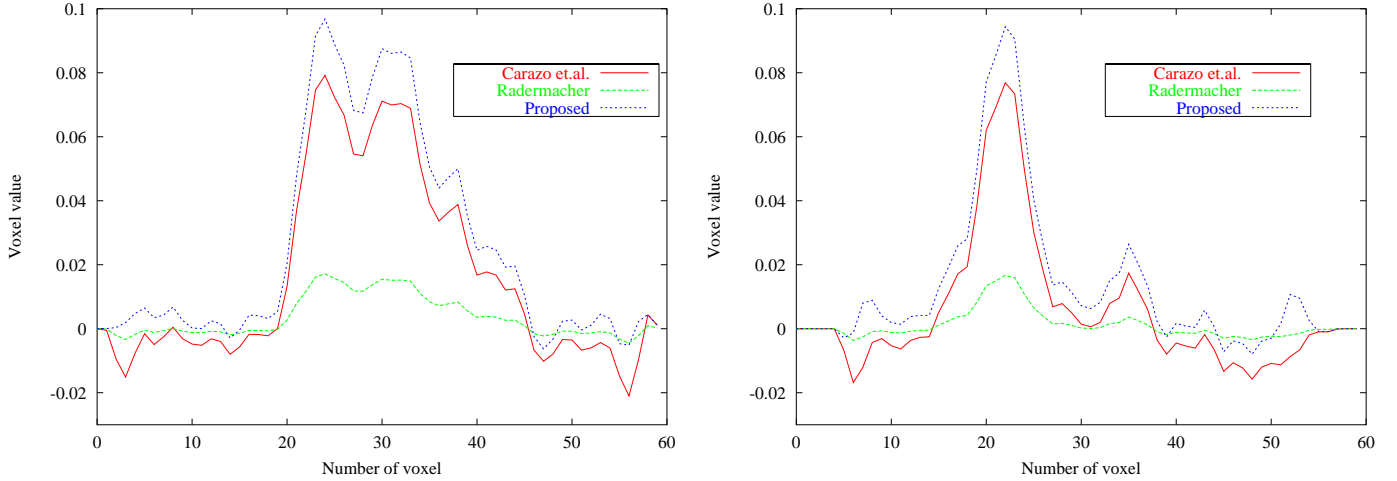
Figure 4: Graphs of the real voxels values at rows 24 and 45 on slice 29 of the reconstructed volumes. The rows used are showed in red in Fig. 3(e). Radermacher procedure results in a poorer dynamic range.
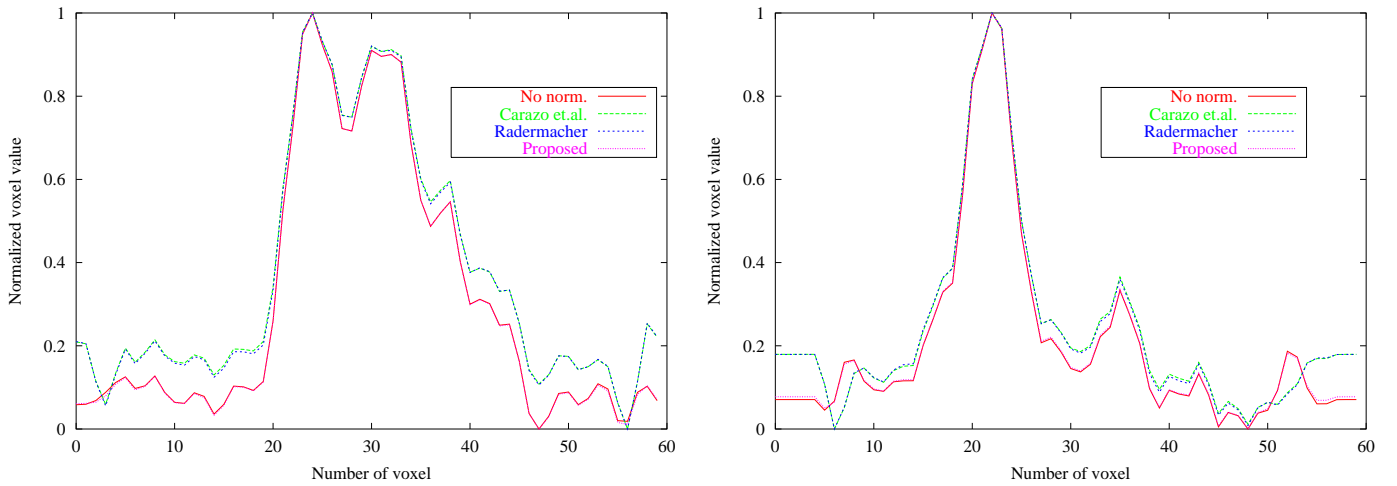

Figure 5: Graphs of the normalized voxels values, between 0 and 1, at rows 24 and 45 on slice 29 of the reconstructed volumes. Clearly the procedures used by Carazo *et. al.* and Radermacher produced the same result. The new proposed normalization procedure give us a reconstruction practically indistinguishable from the reconstruction obtained from non-normalized projections.
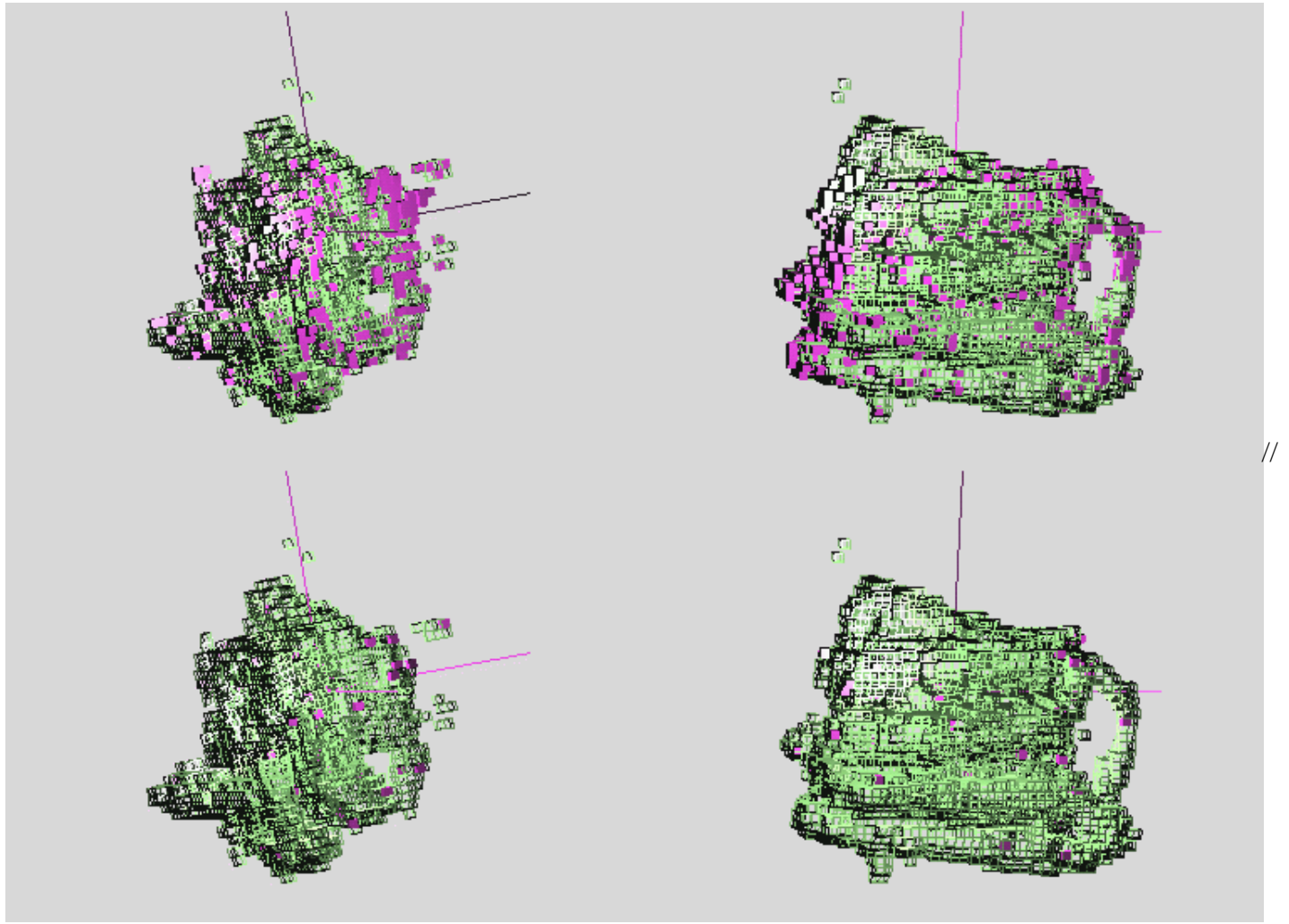
Figure 6: Visualization of the voxels differences between 3D reconstructions. For all four images showed, the green wire represent the 3D reconstruction V_{P_n} (without normalization). The two top images show the different voxels (on violet color) between volumes V_{P_n} and V_A (Carazo *et.al.* procedure). The two bottom images show the different voxels between volumes V_{P_n} and V_C (the new proposed normalization procedure. The volumes were obtained taken 5280 voxels from the histogram density function starting with the highest density [1, p. 268]. These images were rendered using *Scubes* program [18]. The different voxels between volumes V_A, or V_B, and V_{P_n} were 556 voxels, equivalently to 10.5%. The different voxels between volume V_C and V_{P_n} was 43 voxels, or 0.8%.